PoS(DIS2014)231

# Di-hadron production at Jefferson Lab.

**Sérgio Anéfalos Pereira***

*(for the CLAS collaboration)*
*INFN-Frascati - Via Enrico Fermi,40, Frascati, Italy*
*E-mail:* sergio.pereira@lnf.infn.it

Semi-inclusive deep inelastic scattering (SIDIS) has been used extensively in recent years as an important testing ground for QCD. Studies so far have concentrated on better determination of parton distribution functions, distinguishing between the quark and antiquark contributions, and understanding the fragmentation of quarks into hadrons. Hadron pair (di-hadron) SIDIS provides information on the nucleon structure and hadronization dynamics that complement single-hadron SIDIS. Di-hadrons allow the study of low- and high-twist distribution functions and Di-hadron Fragmentation Functions (DiFF). Together with the twist-2 PDFs ($f_1$, $g_1$, $h_1$), the Higher Twist (HT) $e$ and $h_L$ functions are very interesting because they offer insights into the physics of the largely unexplored quark-gluon correlations, which provide access into the dynamics inside hadrons. The CLAS spectrometer, installed in Hall-B at Jefferson Lab, has collected data using the CEBAF 6 GeV longitudinally polarized electron beam on longitudinally polarized solid NH3 targets. Preliminary results on di-hadron beam-, target- and double-spin asymmetries will be presented.

---

*Speaker.

## 1. Introduction

Describing the complex nucleon structure in terms of the partonic degrees of freedom of QCD is one of the main goals of subatomic physics research. Our knowledge on the parton distribution functions (PDFs) and fragmentation functions (FFs), which connect the partonic dynamics to the observed hadrons, has been improved in recent years. Many experiments worldwide are currently trying to pin down various effects related to the nucleon structure through semi-inclusive deep-inelastic scattering (SIDIS), such as HERMES at DESY [1, 2, 3, 4], COMPASS at CERN [5] and at Jefferson Lab [6, 7, 8, 9], with polarized proton-proton collisions as studied at PHENIX, STAR and BRAHMS at RHIC [10, 11, 12], and electron-positron annihilation as studied at Belle at KEK [13, 14]. PDFs provide information about the partonic structure of the hadron giving the probability density for finding a parton (quark or gluon) with a fraction $x$ of the hadron's longitudinal momentum.

In the collinear approximation there are three leading twist PDFs ($f_1$, $g_1$ and $h_1$) and three twist-3 PDFs ($e$, $h_L$ and $g_T$) for different combinations of target (rows in Table 1) and quark (columns in Table 1) polarizations that survive the integration over the transverse momentum. They give a detailed picture of the nucleon in longitudinal momentum space. The higher twist (HT) functions are of interest for several reasons. Most importantly, they offer insights into the physics of the largely unexplored quark-gluon correlations providing access into the dynamics inside hadrons, see, e.g., [15].

| N/q | U | L | T |
|-----|-----|-----|-----|
| U | $f_1$ | | $e$ |
| L | | $g_1$ | $h_L$ |
| T | | $g_T$ | $h_1$ |

**Table 1:** Twist-2 ($f_1$, $g_1$ and $h_1$) and twist-3 ($e$, $h_L$ and $g_T$) parton distribution functions that survive the integration over the transverse momentum. The U,L,T correspond to unpolarized, longitudinally polarized and transversely polarized nucleons (rows) and quarks (columns).

The same PDFs enter into di-hadron production in SIDIS [16, 17, 18, 19, 20, 21, 22]. In fact, the measurement of single-spin asymmetries with longitudinally polarized targets or beams is sensitive, in particular, to the twist-3 chiral-odd distribution functions $e$ and $h_L$, in combination with the chiral-odd interference fragmentation function $H_1^{\sphericalangle}$ [20], making di-hadron production a unique tool to study the higher twist effects appearing as $\sin\phi$ modulations in target or beam spin dependent azimuthal moments of the SIDIS cross section.

## 2. Di-hadron Fragmentation Functions

Consider a reaction

$$\ell(l) + N(P) \to \ell(l') + h_1(P_1) + h_2(P_2) + X, \tag{2.1}$$

where $\ell$ denotes the lepton beam, $N$ the nucleon target, and $h$ the produced hadrons, with the four-vectors in parentheses. The cross section for two-particle inclusive DIS, with final hadron

invariant mass $M_h$ being much smaller than the hard scale $Q^2 = -q^2 \geq 0$ ($q = l - l'$), can be written in terms of modulations in the azimuthal angle $\phi_R$ (in the one-photon exchange approximation and neglecting the lepton mass) [23]. The SIDIS process is defined by the kinematic variables $x = Q^2/2P \cdot q$, $y = P \cdot q/P \cdot l$, $z = P \cdot P_h/P \cdot q$. The $P_h = P_1 + P_2$ and $R = (P_1 - P_2)/2$ are the pair-total and relative momenta, respectively. Following the Trento conventions [24] all relevant angles are defined in [25].

The structure functions can be written in terms of PDFs and Di-hadron Fragmentation Functions (DiFF) in the following way [20]

$$F_{UU,T} = xf_1^q(x)D_1^q(z,\cos\theta,M_h), \tag{2.2}$$

$$F_{UU}^{\cos\phi_R} = -x\frac{|\boldsymbol{R}|\sin\theta}{Q}\frac{1}{z}f_1^q(x)\widetilde{D}^{\sphericalangle q}(z,\cos\theta,M_h), \tag{2.3}$$

$$F_{LU}^{\sin\phi_R} = -x\frac{|\boldsymbol{R}|\sin\theta}{Q}\left[\frac{M}{M_h}xe^q(x)H_1^{\sphericalangle q}(z,\cos\theta,M_h) + \frac{1}{z}f_1^q(x)\widetilde{G}^{\sphericalangle q}(z,\cos\theta,M_h)\right], \tag{2.4}$$

$$F_{UL}^{\sin\phi_R} = -x\frac{|\boldsymbol{R}|\sin\theta}{Q}\left[\frac{M}{M_h}xh_L^q(x)H_1^{\sphericalangle q}(z,\cos\theta,M_h) + \frac{1}{z}g_1^q(x)\widetilde{G}^{\sphericalangle q}(z,\cos\theta,M_h)\right], \tag{2.5}$$

$$F_{LL}^{const} = xg_1^q(x)D_1^q(z,\cos\theta,M_h), \tag{2.6}$$

$$F_{LL}^{\cos\phi_R} = -x\frac{|\boldsymbol{R}|\sin\theta}{Q}\frac{1}{z}g_1^q(x)\widetilde{D}^{\sphericalangle q}(z,\cos\theta,M_h). \tag{2.7}$$

where $\theta$ is the angle between the direction of $P_1$ in the $\pi^+\pi^-$ center-of-mass frame and the direction of $P_h$ in the photon-target rest frame. The subleading-twist fragmentation functions $\widetilde{D}^{\sphericalangle}$ and $\widetilde{G}^{\sphericalangle}$ originate from quark-gluon correlation functions on the fragmentation side. They vanish in the so-called Wandzura–Wilczek approximation [27].

## 3. Results

The data presented were taken with 6 GeV longitudinally-polarized electrons from CEBAF at Jefferson Lab impinging on a longitudinally-polarized solid ammonia target of 0.025 radiation lengths ($NH_3$), immersed in liquid helium [31]. The typical beam current was 7 nA, which, when integrated over the 6 months of data taking, resulted in approximately $50.7 fb^{-1}$ luminosity. The beam polarization averaged 85% and the target proton polarization averaged 80%. Scattered electrons were detected in the CLAS (Cebaf Large Acceptance Spectrometer) detector [28] over the azimuthal angle range of about 18 to 48 degrees.

The kinematic range of the presented data is $4 < W^2 < 9$ GeV and $1 < Q^2 < 6$ GeV$^2$. In the analyzed channel, $ep \rightarrow e'\pi^+\pi^- X$, the final state particles $e'\pi^+\pi^-$ were detected. The beam-, target- and double-spin asymmetries are calculated as following:

$$A_{LU} = \frac{(N^{++} - N^{-+})P_t^- + (N^{+-} - N^{--})P_t^+}{P_B((N^{-+} + N^{++})P_t^- + (N^{--} + N^{+-})P_t^+)}, \tag{3.1}$$

$$A_{UL} = \frac{1}{D_f} \frac{-N^{--} + N^{-+} - N^{+-} + N^{++}}{(N^{-+} + N^{++})P_t^- + (N^{--} + N^{+-})P_t^+}, \tag{3.2}$$

$$A_{LL} = \frac{1}{D_f P_B} \frac{N^{--} - N^{-+} - N^{+-} + N^{++}}{(N^{-+} + N^{++})P_t^- + (N^{--} + N^{+-})P_t^+}, \tag{3.3}$$

where $N^{BT}$ is the number of events for given beam and target polarization directions indicated by the superscripts, respectively. $P_B$, $P_t$ and $D_f$ are the beam polarization, target polarization and dilution factor, respectively.

All the asymmetries were extracted in four bins in $z$ (the fraction of the virtual-photon energy carried by the two hadrons), $x$ and $M_h$ (invariant mass of the two hadrons). The dependencies on each variable are integrated over all the others. All the results shown in the next figures are preliminary. In Fig. 1, the beam-spin asymmetries are shown. Also in Fig. 1 the present results are compared to another CLAS experiment, but with a proton target ($H_2$) instead of a nuclear target ($NH_3$). The results indicate a non-zero asymmetry in all three dependencies. The overall agreement between the two data sets is good and the comparison also shows no evidence of nuclear effects. The extraction of BSA gives access to the $e(x)$ PDF, as can be seen in Eq. 2.4. Target-spin asymmetries are shown in Fig. 2. The $\sin\phi$ and $\sin 2\phi$ dependencies are plotted together. The $\sin 2\phi$ modulation is compatible with zero within the error. The $\sin\phi$ results show non-zero asymmetries in all bins. The TSA increases as $z$ and $M_h$ increase but it seems to decrease as function of $x$. The extraction of the TSA gives access to the $h_L(x)$ PDF, as can be seen in Eq. 2.5. In Fig. 3 the double-spin asymmetries are shown. The top distributions show the constant term of the DSA and the bottom ones, the $\cos\phi$ dependent part. While the $\cos\phi$ asymmetries (bottom plots) are very small (in most of the bins compatible with zero) the constant part (top plots) show big asymmetries up to 45%. From Fig. 3, one can look at the ratio of $A_{LL}^{const}$ and $A_{LL}^{\cos\phi_R}$,

$$\frac{A_{LL}^{const}}{A_{LL}^{\cos\phi_R}} \propto \frac{g_1^q(x) D_1^q(z, \cos\theta, M_h)}{g_1^q(x) \widetilde{D}^{\sphericalangle q}(z, \cos\theta, M_h)}, \tag{3.4}$$

in order to obtain information about the relative weights of $D_1^q$ and $\widetilde{D}^{\sphericalangle q}$. This shows that $\widetilde{D}^{\sphericalangle q}$ is at least one order of magnitude smaller than $D_1^q$, indicating that $\widetilde{G}^{\sphericalangle q}$ is also very small.

The goal of the present work is to extract the PDFs $e$ and $h_L$, that appear multiplied by the interference fragmentation function $H_1^{\sphericalangle}$ in the Eq. 2.4 and 2.5. The interference fragmentation function $H_1^{\sphericalangle}$ has been recently extracted from Belle $e^+/e^-$ measurements [32]. Unfortunately, the $F_{LU}^{\sin\phi_R}$ and $F_{UL}^{\sin\phi_R}$ structure functions contain also another term involving the fragmentation function $\widetilde{G}^{\sphericalangle}$. In the Wandzura-Wilczek approximation [27] the pure twist-3 DiFF, like $\widetilde{G}^{\sphericalangle}$, vanish. In this scenario, the extraction of $e(x)$ and $h_L(x)$ is straightforward, or one has to rely on the measurements of the function $\widetilde{G}^{\sphericalangle}$ from $e^+e^-$ collisions or on the knowledge of the twist-2 PDF $f_1$ and $g_1$.
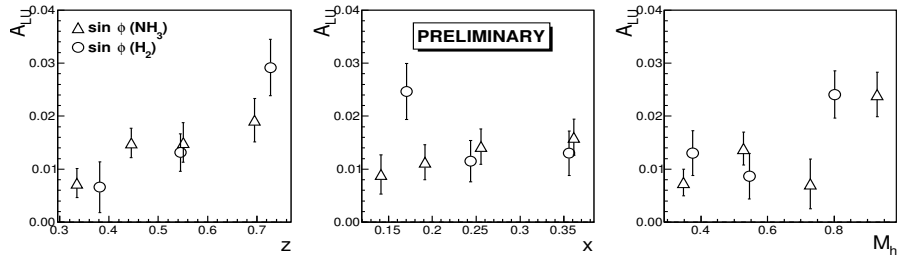
**Figure 1:** Beam-spin asymmetries are shown. The present results (open triangles) are compared with another CLAS experiment (open circles), but with different target ($H_2$) instead of $NH_3$.
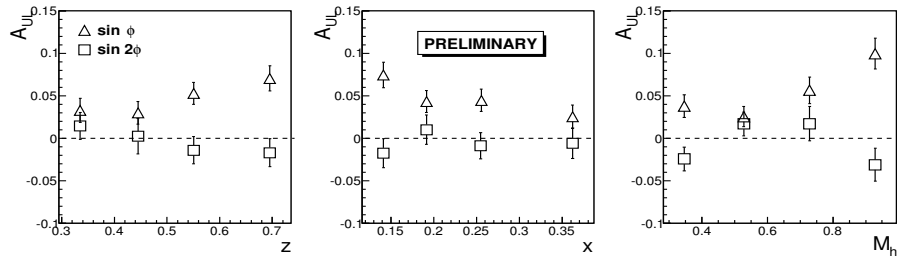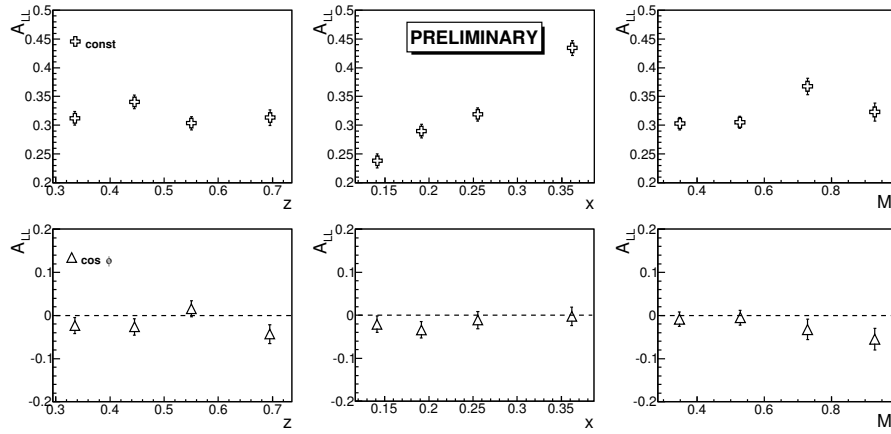


**Figure 2:** Target-spin asymmetries are shown. The $\sin \phi$ (open triangles) and $\sin 2\phi$ (open squares) dependencies are plotted together.

## 4. Conclusion

Di-hadron SIDIS is a very powerful channel in order to access information about the collinear structure of the proton and the CLAS detector at Jefferson Lab is an ideal place to provide such data. These are the first simultaneous measurements of di-hadron $A_{LU}$ , $A_{UL}$ and $A_{LL}$ asymmetries with a non-zero BSA, TSA and DSA for $\pi^+\pi^-$ pairs. The comparison between unpolarized $H_2$ and longitudinally-polarized $NH_3$ target $A_{LU}$ asymmetries indicates the absence of nuclear effects.

## References

[1] A. Airapetian et al., Phys. Rev. Lett. **84** (2000) 4047, hep-ex/9910062.

[2] A. Airapetian et al., Phys. Rev. D**64** (2001) 097101, hep-ex/0104005.

[3] A. Airapetian et al., Phys. Rev. Lett. **94** (2005) 012002, hep-ex/0408013.

[4] A. Airapetian et al., Phys. Lett. B**648** (2007) 164, hep-ex/0612059.

[5] V.Y. Alexakhin et al., Phys. Rev. Lett. **94** (2005) 202002, hep-ex/0503002.

[6] H. Avakian et al., Phys. Rev. D**69** (2004) 112004, hep-ex/0301005.

[7] H. Avakian et al., AIP Conf. Proc. **792** (2005) 945, nucl-ex/0509032.

[8] H. Mkrtchyan et al., Phys. Lett. B**665** (2008) 20, hep-ph/0709.3020.

[9] M. Osipenko et al., Phys. Rev. D**80** (2009) 032004, hep-ex/0809.1153.

PoS(DIS2014)231

**Figure 3:** The double-spin asymmetries are shown. The top distributions show the constant term of the DSA (open crosses) and the bottom ones the $\cos\phi$ dependent part (open triangles).

[10] M. Chiu, AIP Conf. Proc. **915** (2007) 539, nucl-ex/0701031.

[11] J. Adams et al., Phys. Rev. Lett. **92** (2004) 171801, hep-ex/0310058.

[12] I. Arsene et al., Phys. Rev. Lett. **101** (2008) 042001, nucl-ex/0801.1078.

[13] K. Abe et al., Phys. Rev. Lett. **96** (2006) 232002, hep-ex/0507063.

[14] A. Vossen et al., Phys.Rev.Lett. **107** (2011) 072004.

[15] R.L. Jaffe, Comments Nucl. Part. Phys. **19** (1990) 239.

[16] R.L. Jaffe, X.m. Jin and J. Tang, Phys. Rev. Lett. **80** (1998) 1166, hep-ph/9709322.

[17] A. Bianconi et al., Phys. Rev. D**62** (2000) 034008, hep-ph/9907475.

[18] M. Radici, R. Jakob and A. Bianconi, Phys. Rev. D**65** (2002) 074031, hep-ph/0110252.

[19] A. Bacchetta and M. Radici, Phys. Rev. D**67** (2003) 094002, hep-ph/0212300.

[20] A. Bacchetta and M. Radici, Phys. Rev. D**69** (2004) 074026, hep-ph/0311173.

[21] A. Bacchetta and M. Radici, Phys. Rev. D**74** (2006) 114007, hep-ph/0608037.

[22] F.A. Ceccopieri, M. Radici and A. Bacchetta,Phys. Lett. B**650** (2007) 81, hep-ph/0703265.

[23] A. Bacchetta et al., JHEP **02** (2007) 093, hep-ph/0611265.

[24] A. Bacchetta et al., Phys. Rev. D**70** (2004) 117504, hep-ph/0410050.

[25] A. Airapetian et al., JHEP **06** (2008) 017, 0803.2367.

[26] M. Diehl and S. Sapeta, Eur. Phys. J. C**41** (2005) 515, hep-ph/0503023.

[27] S. Wandzura and F. Wilczek, Phys. Lett. B**72** (1977) 195.

[28] B. A. Mecking *et al.*, Nucl. Instrum. Methods A **503**, 444 (2003).

[29] D. I. Sober *et al.*, Nucl. Instrum. Methods A **440**, 263 (2000).

[30] C. D. Keith *et al.*, Nucl. Instrum. Methods A **501**, 327 (2003).

[31] C.D. Keith et al., Nucl. Instr. Meth. **501**, 327 (2003).

[32] A. Courtoy *et al.*, Phys. Rev. D**85** (2012) 114023.